

# Probing the Surface Hydration of Nonfouling Zwitterionic and PEG Materials in Contact with Proteins

Chuan Leng,<sup>†</sup> Hsiang-Chieh Hung,<sup>‡</sup> Shuwen Sun,<sup>†</sup> Dayang Wang,<sup>\*,§</sup> Yuting Li,<sup>‡</sup> Shaoyi Jiang,<sup>\*,‡</sup> and Zhan Chen<sup>\*,†</sup>

<sup>†</sup>Department of Chemistry, University of Michigan, Ann Arbor, Michigan 48109, United States

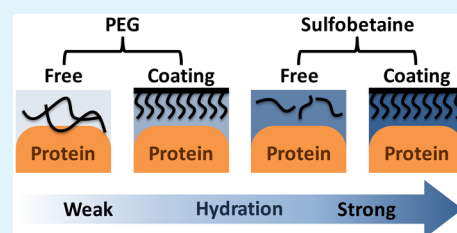
<sup>‡</sup>Department of Chemical Engineering, University of Washington, Seattle, Washington 98195, United States

<sup>§</sup>Ian Wark Research Institute, University of South Australia, Mawson Lakes, SA 5095, Australia

## Supporting Information

**ABSTRACT:** Zwitterionic polymers and poly(ethylene glycol) (PEG) have been reported as promising nonfouling materials, and strong surface hydration has been proposed as a significant contributor to the nonfouling mechanism. Better understanding of the similarity and difference between these two types of materials in terms of hydration and protein interaction will benefit the design of new and effective nonfouling materials. In this study, sum frequency generation (SFG) vibrational spectroscopy was applied for in situ and real-time assessment of the surface hydration of the sulfobetaine methacrylate (SBMA) and oligo(ethylene glycol) methacrylate (OEGMA) polymer brushes, denoted as pSBMA and pOEGMA, in contact with proteins. Whereas a majority of strongly hydrogen-bonded water was observed at both pSBMA and pOEGMA surfaces, upon contact with proteins, the surface hydration of pSBMA remained unaffected, but the water ordering at the pOEGMA surface was disturbed. The effects of free sulfobetaine, free PEG chains with two different molecular weights, and PEG coated gold nanoparticles on the surface hydration of proteins were investigated. The results indicated that free sulfobetaine could strengthen the protein hydration layer, but free PEG chains greatly disrupt the protein hydration layer and likely directly interact with the protein molecules. In contrast to free PEG, the PEG chains anchored on the nanoparticles behave similarly to the pOEGMA surface and could induce strong hydrogen bonding of the water molecules at the protein surfaces.

**KEYWORDS:** nonfouling materials, sum frequency generation (SFG) vibrational spectroscopy, zwitterionic polymer, sulfobetaine, poly(ethylene glycol) (PEG), gold nanoparticles, hydration, hydrogen bonding



## INTRODUCTION

Nonfouling materials have been extensively investigated for a wide spectrum of applications ranging from marine industry to biomedical engineering.<sup>1–6</sup> Two types of the most widely studied nonfouling materials are zwitterionic polymers<sup>7</sup> and poly(ethylene glycol) (PEG).<sup>8</sup> It is believed that the nonfouling property of these materials results from their strong surface hydration, which is formed at the zwitterionic polymer surfaces through electrostatic-induced hydrogen bonding, and at the PEG surfaces through hydrogen bonding between water molecules and the ether oxygen atoms.<sup>9–11</sup> The tightly bound hydration layer is theorized to act as a physical and energy barrier, and the water molecules are difficult to be replaced by biomolecules and organisms. However, this straightforward correlation between the nonfouling behavior of a material and its surface hydration may be questionable, because the presence of biological molecules such as proteins or organisms complicates the adsorption behavior and the interfacial water structure.<sup>12</sup> A deeper understanding of the nonfouling performance of a material needs a comprehensive molecular picture underlying the hydration at the material surface and the protein surface, which, however, has not been completely established. Therefore, it is imperative to probe the

local water structures at both nonfouling material and protein surfaces and especially their temporal evolution when the nonfouling materials are brought to interact with the proteins in water or vice versa.

Zwitterionic polymers and PEG differ in molecular structure, which may result in their different hydration properties. Molecular dynamics simulation results suggested that there are hydrophobic interactions between PEG and proteins.<sup>13</sup> Because of the hydrophobic interactions, PEG can block the active sites of enzymes, leading to reduction in the catalytic activity of PEG-enzyme conjugates. In contrast, the bioactivity of enzymes can be retained or even improved after conjugation with zwitterionic polymers, because the superhydrophilicity of the zwitterionic polymers offers a hydration environment that favors enzyme–substrate interaction.<sup>14</sup> Further, the surface coatings of zwitterionic polymers exhibit better in vivo performance than PEG, including minimal biomolecule binding,<sup>15</sup> resistance to foreign body reaction,<sup>16</sup> and long circulation.<sup>17</sup> Because their molecular structures are distinctly

Received: June 24, 2015

Accepted: July 10, 2015

Published: July 10, 2015

different, it is not a surprise that zwitterionic polymers and PEG have different mechanisms to interact with water, proteins, and organisms. This hypothesis is plausible but has not been validated by direct experimental evidence so far. In this context, it is of essential importance to probe the local water structures at the zwitterionic polymer and PEG surfaces and their responses to the presence of protein molecules. We believe that this fundamental study will allow better design and tailoring of the nonfouling performance of materials in a variety of technical applications, for instance, in biomedicine, where contact with biological environments containing proteins or organisms is inevitable at the material surfaces.

Sum frequency generation (SFG) vibrational spectroscopy is a surface-sensitive and in situ vibrational spectroscopic technique, providing information about chemical structures at the molecular level.<sup>18–20</sup> It has been extensively applied to study the molecular structures of polymers<sup>21</sup> and biomolecules<sup>22,23</sup> at various interfaces and has proven particularly powerful in revealing polymer/water interfacial structures<sup>24,25</sup> in ambient environments. Furthermore, the detailed structural information on interfacial water can be extracted from SFG data.<sup>26–30</sup>

In this work, SFG spectroscopy was applied to systematically study the surface hydration of the polymer brushes of sulfobetaine methacrylate (SBMA) and oligo(ethylene glycol) methacrylate (OEGMA), denoted as pSBMA and pOEGMA, anchored on silica surfaces (Figure 1A) in the absence and presence of proteins (Figure 1B). The SFG spectra of water at the polymer surfaces were taken before, during, and after contacting several protein solutions, and the time-dependent SFG signals of the interfacial water were monitored to probe the structural changes of water upon contact with the protein

solutions. The SFG results revealed that pSBMA and pOEGMA surfaces showed different surface hydrations upon contact with the protein solutions. In addition, the effects of sulfobetaine (SB), PEGs with molecular weight of 300 and 2000 (PEG-300 and PEG-2000), and PEG-2000-coated gold nanoparticles (PEG-2000-AuNP) (Figure 1C) on the surface hydration of proteins were investigated (Figure 1D) with SFG spectroscopy, which further elucidated the different hydration between SB and PEG in contact with proteins.

## EXPERIMENTAL SECTION

Bovine serum albumin (BSA, 99%), lysozyme (90%), fibrinogen (Type I-S, 65–85%, may contain 10% sodium citrate and 15% sodium chloride), fluorescein isothiocyanate labeled BSA (FITC-BSA), dimethylethylammoniumpropanesulfonate (sulfobetaine, SB), PEG-300, PEG-2000, PEG-2000-AuNP (diameter = 20 nm, optical density (OD) = 50) dispersed in water, and phosphate buffered saline (PBS, prepared from  $\text{Na}_2\text{HPO}_4$  and  $\text{KH}_2\text{PO}_4$ , contains 11.9 mM phosphates, 137 mM NaCl, and 2.7 mM KCl, pH =  $7.4 \pm 0.1$ ) were purchased from Sigma-Aldrich. Deuterated polystyrene (d8-PS) ( $M_w$  of ca. 207 500 g/mol) was purchased from Polymer Source Inc. Right angle  $\text{SiO}_2$  and  $\text{CaF}_2$  prisms were purchased from Altos Photonics. Millipore water was used in all experiments.

The brushes of pSBMA and pOEGMA were grown on  $\text{SiO}_2$  prisms (Figure 1A) via atomic transfer radical polymerization (ATRP) according to previous reports.<sup>31,32</sup> The thicknesses of the identical polymer brushes prepared on silicon wafers were measured to be 25–30 nm by an alpha-SE ellipsometer (J. A. Woollam). The hydrophilicity of the polymer coatings was assessed by static water contact angles measured with a CAM 100 contact angle goniometer (KSV Instruments).

To test the protein adsorption on the polymer surfaces, the pSBMA and pOEGMA samples were immersed into the PBS solution of FITC-BSA (5 mg/mL) for 1 h, followed by rinsing with water and drying with  $\text{N}_2$  flow. The surface adsorption of FITC-BSA molecules was assessed with an inverted fluorescence microscope (Olympus, Melville, NY) equipped with a xenon arc lamp (Sutter Instrument Co., Novato, CA) and an electron multiplier CCD camera (Hamamatsu, Bridgewater, NJ). A bare silica substrate was used as a control.

To probe the water structure at the polymer brush/water interfaces in the absence and presence of proteins, the polymer brush samples were placed in water and the aqueous solutions of BSA, lysozyme, and fibrinogen (1.0 mg/mL), respectively (Figure 1B). The SFG spectroscopy was implemented according to the protocol reported previously.<sup>33</sup> Briefly, the visible and infrared (IR) input beams penetrated a right angle prism and overlapped spatially and temporally at the sample surface or interface. The incident angles of the visible and IR beams were  $60^\circ$  and  $54^\circ$  with respect to the surface normal, and the pulse energies of the visible and IR beams were 30 and 100  $\mu\text{J}$ , respectively. The reflected SFG signal was collected by a monochromator along with a photomultiplier tube. All SFG spectra were collected using the ssp (s-polarized sum frequency output, s-polarized visible input, and p-polarized IR input) polarization combination.<sup>34</sup>

To study the effects of proteins on the surface hydration of the polymers, we adopted the following procedure. The polymer sample was first measured with SFG in air from 2800 to 3100  $\text{cm}^{-1}$  (for C–H signal) and then placed in water for another SFG measurement from 2800 to 3600  $\text{cm}^{-1}$  (for C–H and O–H signals). Time-dependent SFG signal at the wavenumber of OH stretching vibration (around 3200  $\text{cm}^{-1}$ ) then was monitored while water was switched to a protein solution in situ. When the OH signal at the protein solution interface was stable, an SFG spectrum was taken from 2800 to 3600  $\text{cm}^{-1}$ . Finally, the sample was rinsed with water with a regular wash bottle, dried under  $\text{N}_2$ , and measured with SFG in air and water again.

To study the effects of SB, PEG-300, PEG-2000, and PEG-2000-AuNPs in water on the surface hydration of proteins, a protein layer was physically adsorbed on the prism. First, a d8-PS solution in

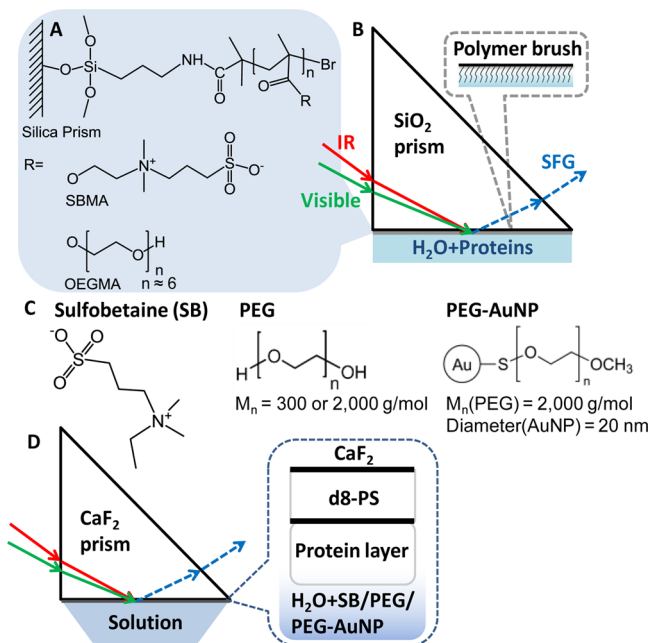


**Figure 1.** (A) Molecular structures of pSBMA and pOEGMA brushes anchored on silica surfaces. (B) SFG measurement of a polymer coating on a right-angle  $\text{SiO}_2$  prism in contact with a protein solution. (C) Molecular structures of SB, PEG-300, PEG-2000, and PEG-2000-AuNPs. (D) SFG measurement of a protein layer physically adsorbed on a deuterated polystyrene (d8-PS) coated  $\text{CaF}_2$  prism in contact with an SB, PEG-300, PEG-2000, or PEG-2000-AuNP solution.

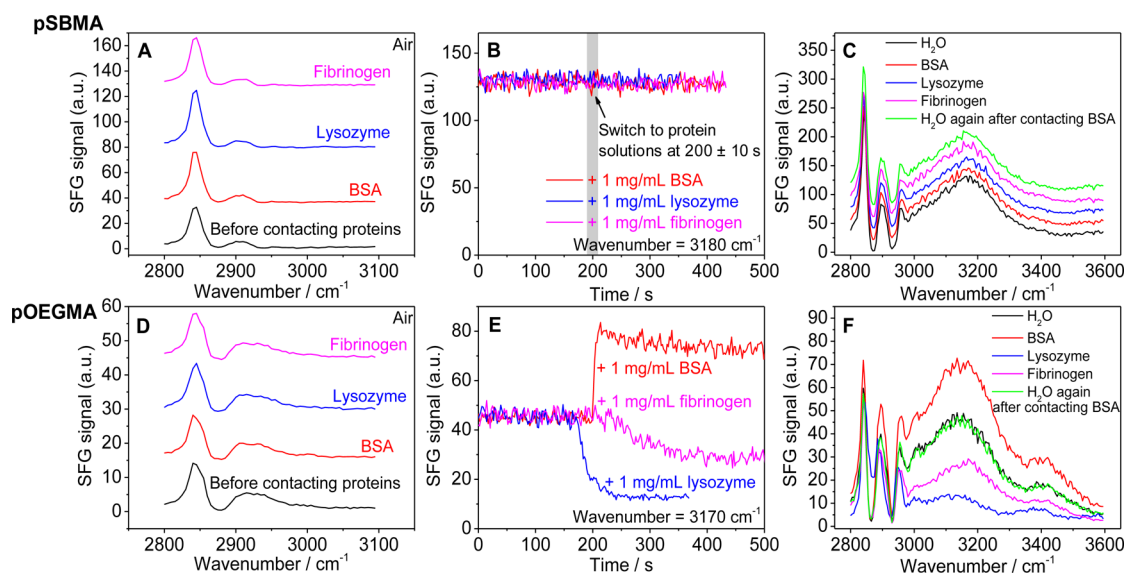


**Figure 2.** SFG signals of (A–C) pSBMA and (D–F) pOEGMA before, during, and after contacting the solutions of BSA, lysozyme, and fibrinogen. SFG spectra of (A) pSBMA and (D) pOEGMA were collected in air before and after contacting each protein solution. Time-dependent water signals of (B) pSBMA and (E) pOEGMA were monitored in situ as the aqueous phase was switched from water to each protein solution. SFG spectra of (C) pSBMA and (F) pOEGMA in contact with water and the protein solutions were also collected. The spectra in (A), (C), and (D) are stacked and offset by vertical translation for a clear view.

toluene (1% w/w) was spin-coated on a clean CaF<sub>2</sub> prism at 3000 rpm for 30 s with a P-6000 spin coater (Speedline Technologies). Second, the d8-PS coated prisms were immersed in the PBS solutions of BSA, lysozyme, and fibrinogen (5.0 mg/mL), respectively, for 30 min. Third, the protein coatings on the prisms were rinsed with water and dried under N<sub>2</sub>. The presence of d8-PS and the proteins was confirmed by water contact angle measurements (Supporting Information Table S1). The protein surfaces were then measured with SFG in contact with water and the aqueous solutions of SB (0.5 M), PEG-300 (0.5 M), PEG-2000 (0.08 M), or PEG-2000-AuNP (OD = 5) (Figure 1D).

## RESULTS AND DISCUSSION

**Surface Characterization and Hydration of pSBMA and pOEGMA.** To study the surface hydration of nonfouling materials, the as-prepared pSBMA and pOEGMA were selected in this work considering the following factors: First, proteins can adsorb onto charged surfaces through Coulomb interaction.<sup>35–39</sup> Both pSBMA and pOEGMA herein are overall neutral, so Coulomb interaction-induced protein adsorption is excluded. Second, the hydrophilicity and nonfouling properties of the polymer brushes are affected by their thicknesses.<sup>31,32,40</sup> The pSBMA and pOEGMA films with a thickness of 25–30 nm herein demonstrated strong resistance to protein adsorption.<sup>31,32</sup> Third, high packing density is crucial to the nonfouling performance of the polymer brushes.<sup>31,41</sup> Here, to ensure the high packing density, the initiators were anchored on the silica surface to form a self-assembled monolayer with high density.<sup>31,32</sup> Fourth, the polymer chemical composition influences their nonfouling properties. For example, ethylene glycol (EG) oligomer molecules anchored on surfaces with six or more EG units demonstrate strong protein resistance.<sup>42</sup> The nonfouling property of polymers made from carboxybetaine is affected by environmental pH, whereas that of sulfobetaine is independent of pH.<sup>39</sup> Therefore, pSBMA and pOEGMA (EG unit = 6) were selected for study in this work.

The surface hydrophobic/hydrophilic properties of the polymer brushes studied here were characterized by sessile drop measurements. As shown in Supporting Information Figure S1, the static water contact angles of the pSBMA and pOEGMA brushes anchored on silica substrates were measured to be  $20 \pm 1^\circ$  and  $42 \pm 1^\circ$ , respectively, which agree with those reported in the literature,<sup>31,40,43–45</sup> and were smaller than those of the commonly used polymers such as poly(methyl methacrylate),<sup>46</sup> polyethylene terephthalate,<sup>46</sup> polycarbonate,<sup>46</sup> polyvinyl chloride,<sup>47</sup> poly(dimethylsiloxane),<sup>47</sup> or polystyrene.<sup>48</sup> The water contact angle of the pSBMA surfaces is noticeably smaller than that of the pOEGMA surfaces, suggesting that the zwitterionic groups of the pSBMA brushes can interact more strongly with water for more effective surface hydration than the ethylene oxide groups of the pOEGMA brushes.

The resistance of pSBMA and pOEGMA to protein adsorption determined by surface plasmon resonance and ellipsometry measurements has been well-documented.<sup>8,31,32,49,50</sup> To verify the nonfouling performance of the as-prepared pSBMA and pOEGMA, FITC-BSA was used as a model protein, and its adsorption on the polymer brushes and a bare silica substrate (as a control sample) was measured with fluorescence microscopy. As shown in Supporting Information Figure S2, whereas strong FITC-BSA adsorption on bare silica surface was detected, no protein adsorption was observed on pSBMA or pOEGMA, indicating that both of the polymer surfaces were effectively resistant to protein adsorption in water as reported.<sup>31,32</sup> This provides the basis for the interpretation of the SFG results below.

Figure 2 shows the SFG spectra collected from the pSBMA and pOEGMA surfaces in air, in water, and in various protein solutions. The time-dependent SFG signals detected from the interfaces between the polymers and aqueous media before and after the addition of the proteins to the aqueous media are also shown. In air, both the pSBMA and the pOEGMA surfaces show a strong peak at  $2845 \text{ cm}^{-1}$  and a weak peak at  $2920 \text{ cm}^{-1}$

from symmetric and asymmetric stretching modes of the methylene groups<sup>34</sup> in the polymer backbone and/or side chains (Figure 2A and D, black curves), indicative of good ordering of the polymers at the polymer/air interfaces. The polymer surfaces also show a strong C–H signal below 3000  $\text{cm}^{-1}$  in water, indicative of good ordering of the polymers at the polymer/water interfaces as well (Figure 2C and F, black curves). The water signal above 3000  $\text{cm}^{-1}$  at the pSBMA surface consists of only one band centered around 3180  $\text{cm}^{-1}$  with a hardly observable signal at 3400  $\text{cm}^{-1}$ . Differently, the water signal at the pOEGMA surface is dominated by the band centered around 3170  $\text{cm}^{-1}$  with a shoulder around 3400  $\text{cm}^{-1}$ , which are assigned to strongly and weakly hydrogen-bonded water molecules,<sup>29</sup> respectively. Thus, the majority of the ordered water molecules are associated via strong hydrogen bonding at both the pSBMA and the pOEGMA surfaces, but some water molecules via weak hydrogen bonding at the pOEGMA surface. The different water structures at the pSBMA and pOEGMA surfaces may reflect the differences in hydrogen-bonding mechanisms. Water molecules form hydrogen bonds with the hydrophilic zwitterionic groups in pSBMA or the oxygen atoms in the repeating units of the OEG chains, while the former is enhanced by electrostatic attraction.

**Impact of Proteins on the Surface Hydration of pSBMA and pOEGMA.** To study the impact of proteins on polymer hydration, proteins were prepared in water instead of PBS because the ionic strength of PBS is high enough to change the interfacial water structure and affect the SFG water signal (Supporting Information Figure S3). Moreover, we excluded the possibility that the low concentration of salts in the protein solutions (e.g., 150 mg/L (2.6 mM) sodium chloride and 100 mg/L (0.47 mM) monosodium citrate) may affect the SFG signal of water (Supporting Information Figure S3). Here, we selected BSA, lysozyme, and fibrinogen to represent typical proteins because they have a wide range of molecular weights and isoelectric points (Supporting Information Table S2).

The SFG signal intensity of water was monitored in real time when the aqueous phase was switched from water to a protein solution at the polymer surface (Figure 2B and E). For pSBMA, the intensity of the water SFG signal at 3180  $\text{cm}^{-1}$  remains the same when the aqueous phase is switched from water to different protein solutions (Figure 2B), indicating that the strongly hydrogen-bonded water structure is hardly disturbed by proteins. The SFG spectra collected from the pSBMA/protein solution interfaces are almost identical to those taken at the pSBMA/water interface, indicating the same interfacial polymer and water structures at the pSBMA/protein solution and pSBMA/water interfaces (Figure 2C). This indicates that the interfacial water molecules are strongly bonded with pSBMA and cannot be disturbed by the protein molecules under the current experimental condition. After the surface was rinsed with water, the SFG spectra of the pSBMA surface collected in air and water are identical to those obtained from the original pSBMA surface before contacting protein solutions, indicating no change of the polymer surface structure and no adsorption of the proteins onto the pSBMA surface (Figure 2A,C, and Supporting Information Figure S4A).

Different from pSBMA, the water signal at 3170  $\text{cm}^{-1}$  at the pOEGMA surface becomes either stronger or weaker upon contacting protein solutions, indicating a noticeable impact of the presence of proteins on the water molecules at the pOEGMA surface (Figure 2E). After about 150 s, the water

signal at the pOEGMA surface in the protein solutions reaches a plateau. When the water signal did not exhibit further change, SFG spectra were taken at the pOEGMA/protein solution interfaces. The C–H stretching signals taken at the pOEGMA/protein solution interfaces are similar to those at the pOEGMA/water interface (Figure 2F), indicative of little change in the polymer structures upon contact with the proteins and no preferred ordering of the proteins at the polymer surface. However, the contact with proteins causes noticeably different changes in the water signal intensity, suggesting that the ordering of the water molecules adjacent to the polymer surface is very sensitive to the presence of proteins and the protein nature. Note that whereas the water signal intensity at 3170  $\text{cm}^{-1}$  greatly changes upon contacting each protein solution, the change of the peak area of the 3400  $\text{cm}^{-1}$  component is much smaller than that of the 3170  $\text{cm}^{-1}$  component. This suggests that protein molecules near the pOEGMA surface primarily disturb the structural ordering of the strongly hydrogen-bonded water molecules that most likely hydrogen-bonded with the oxygen atoms on the OEG chains. After the pOEGMA surface was removed from the protein solutions and rinsed with water, their SFG spectra in air show the same signals as that taken before contacting the protein solutions (Figure 2D). Furthermore, the water signal at the pOEGMA surface is completely recovered when the surface was placed in pure water again (Figure 2F and Supporting Information Figure S4B). These data demonstrate little change in the polymer structures and negligible protein adsorption, which is consistent with the aforementioned fluorescence measurements.

A clean silica surface interacting with the proteins was monitored as a control. The water contact angle of the silica surface was measured to be less than 5°. As shown in Figure S5 in the Supporting Information, there was no SFG signal visible in the C–H stretching frequency region in air. After contacting the protein solutions and being rinsed with water, the surface in air showed peaks at 2880 and 2925  $\text{cm}^{-1}$ , which were assigned to the hydrophobic groups of the proteins at the air interface (Supporting Information Figure S5A), indicating the protein adsorption on the silica surface.<sup>51,52</sup> The water signal was monitored when the aqueous phase in contact with the silica surface was switched from water to the protein solutions. As shown in Supporting Information Figure S5B, the time-dependent SFG water signal intensity increased or decreased upon contacting protein solutions, due to the disturbance of the interfacial water structure by the proteins. These data were similar to those obtained with pOEGMA (Figure 2E). However, after the surface was rinsed with water and placed in water again, the interfacial water signal detected at the silica/water interface could not be recovered to its original intensity due to the irreversible protein adsorption (Supporting Information Figure S5C).

The above SFG results highlight that pSBMA, pOEGMA, and silica surfaces exhibit different surface hydration and protein adsorption behavior. A layer of strongly hydrogen-bonded interfacial water molecules protects the pSBMA surface from protein contact. At the pOEGMA surface, the proteins can disturb the interfacial water structure and may possibly directly interact with the polymer surface. However, proteins can be rinsed off from the pOEGMA surface, suggesting that the OEG chains interact with water more strongly than with the proteins, leaving behind no proteins adsorbed on the pOEGMA

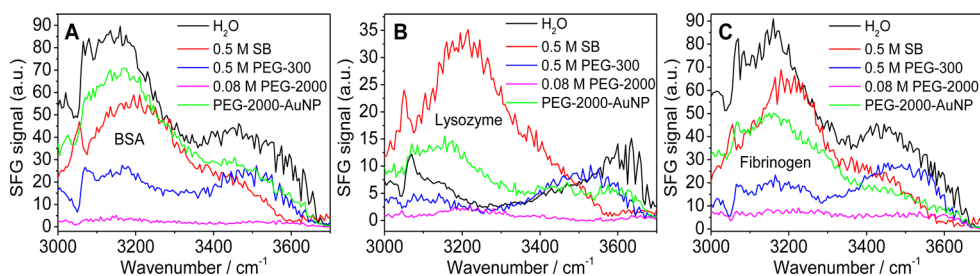


**Figure 3.** SFG spectra of (A) BSA, (B) lysozyme, and (C) fibrinogen adsorbed on d8-PS coatings in contact with water and aqueous solutions of SB (0.5 M), PEG-300 (0.5 M), PEG-2000 (0.08 M), and PEG-2000-AuNPs (OD = 5).

surface. For silica, the proteins change the interfacial water structure and irreversibly adsorb onto the surface.

#### Impact of SB and PEG on Protein Surface Hydration.

To further reveal the difference in surface hydration between zwitterionic materials and PEG, we applied SFG to investigate the effects of the structural unit of pSBMA and pOEGMA, SB, and PEG-300 (Figure 1C), on the surface hydration of proteins. Figure 3 demonstrates that the water structures at the protein surfaces are dependent on the protein nature. The signal centered at about 3200  $\text{cm}^{-1}$  dominates the SFG water spectra at the BSA and fibrinogen surfaces, whereas the signal around 3500  $\text{cm}^{-1}$  is stronger at the lysozyme/water interface. The observation on the lysozyme surface is consistent with the results presented in Figure 2E and F, which shows that lysozyme (originally with weak hydration) affects the hydration layer of pOEGMA more than BSA and fibrinogen. The different features of the water spectra should be correlated with the different conformation and charge of the proteins and the different ways in which the proteins orient surface water molecules. For example, lysozyme is known to be more rigid than the other two proteins and has a higher isoelectric point. The detailed study of the correlation of the water structures with the protein nature, however, is beyond the scope of this work. The present work focuses on the water signal change at the protein surfaces after SB and PEG are introduced into the surrounding environment of the protein surfaces. Regardless of the different water structures at the protein surfaces, the surface hydration of different types of proteins is affected by SB or PEG-300 in a rather similar way, as discussed below.

When the protein surfaces are placed in contact with a 0.5 M SB solution, the SFG water spectra are dominated by the signal centered at about 3200  $\text{cm}^{-1}$  for all three proteins (Figure 3, red curves), which is assigned to strongly hydrogen-bonded water molecules.<sup>29</sup> As suggested by Figure 2C, strongly hydrogen-bonded water molecules are present at the pSBMA/water and pSBMA/protein solution interfaces, which are hardly affected by the proteins. Similarly, free SB molecules are expected to have strongly hydrogen-bonded water molecules in their hydration shells. When they are in close proximity to the protein layers, their hydration shells remain hardly changed. The strong hydration shells on the SB molecules effectively prevent the near-surface contact between the proteins and SB molecules. This agrees with the results presented in Figure 2. To further reveal the importance of a zwitterion (inner salt) in surface hydration rather than independent ions, a salt solution of ammonium sulfate with the same concentration (0.5 M) was investigated as a control. As shown in Supporting Information Figure S6, for all of the proteins, the interfacial water signals decreased to almost zero while in contact with the ammonium sulfate solution. Different

from SB, here the ammonium and sulfate ions can separately interact with the charged domains of the proteins; therefore, the hydration of the proteins is significantly disrupted.

However, when the protein surfaces were in contact with the PEG-300 solution, the SFG signal centered at ca. 3500  $\text{cm}^{-1}$ , contributed from weakly hydrogen-bonded or less coordinated water,<sup>29</sup> becomes noticeably stronger than the signal around 3200  $\text{cm}^{-1}$  (Figure 3, blue curves) for all three types of proteins, although both of these signals were largely reduced. This is different from the water signals observed at the BSA/water and fibrinogen/water interfaces (Figure 3A and C, black curves), and is also different from that observed from the pOEGMA/water interface (Figure 2F, black curve). PEG is a hydrogen-bond acceptor, and it can be envisioned that PEG/water hydrogen bonds are formed at the cost of the hydrogen bonds between water molecules. Comparison of the SFG signals at 3200  $\text{cm}^{-1}$  at the protein/water interfaces in the absence and presence of PEG-300 suggests that PEG-300 effectively breaks the strongly hydrogen-bonded water, but has less effect on the weakly hydrogen-bonded water. Distinct from the pOEGMA/water interface in the presence of proteins in water, at which the majority of water molecules are strongly hydrogen-bonded, at the protein/water interfaces in the presence of PEG-300 molecules, the majority of water molecules are weakly hydrogen-bonded. Thereby, we believe that free PEG molecules in water behave differently from PEG molecules anchored on a solid surface.

Free PEG molecules are expected to interact with proteins via hydrophobic interaction between the  $\text{CH}_2$  moieties on their backbones and the hydrophobic parts of proteins.<sup>13,53</sup> To confirm the effect of the hydrophobic interaction between PEG and proteins, here the protein layers were brought into contact with the aqueous solution of PEG-2000, the concentration of which was 0.08 M to achieve the same concentration of ethylene glycol unit of PEG-300 at 0.5 M. Figure 3 shows that the water signals at the protein/water interfaces decrease to almost zero upon contact with PEG-2000. This suggests that PEG-2000 substantially disrupts the hydration layer(s) around the proteins and interacts with the proteins more strongly than PEG-300. It is possible that the long PEG chains can even wrap the protein molecules. Taking into account the results shown in Figure 2E and F, the studies of the hydration at the pOEGMA surface and at the protein layers confirm the direct interaction between PEG and proteins.

The comparison between Figures 2 and 3 indicates that free PEG and surface-bound PEG may affect the protein hydration differently. To further test this, PEG-2000-AuNP was introduced to interact with the protein layers in water to compare with free PEG-300 and PEG-2000 molecules. As shown in Figure 3 (green curves), the water signal at 3200  $\text{cm}^{-1}$

remains stronger than that at  $3400\text{ cm}^{-1}$ , particularly for the lysozyme surface, at which the original signal at  $3200\text{ cm}^{-1}$  is weaker in contact with water (Figure 3B, black curve). This result indicates that, different from free PEG, the PEG chains tethered on the nanoparticles can form and align strongly hydrogen-bonded water molecules adjacent to the protein surfaces, which is similar to the pOEGMA surface (Figure 2F). Similar to those coated on planar surfaces, the PEG chains tethered on nanoparticles are closely packed with most of the hydrophobic  $\text{CH}_2$  groups buried in the film, and have limited freedom to change conformation to interact with proteins directly, which, therefore, yields strong hydration shells enclosing the PEG-2000-AuNPs to prevent the near-surface contact of the nanoparticles with proteins.

The impact of SB, PEG-300, PEG-2000, and PEG-2000-AuNPs on the surface hydration of  $\text{CaF}_2$  without the proteins was investigated for comparison. As shown in Supporting Information Figure S7, the spectrum taken with the presence of SB shows a strong band at  $3200\text{ cm}^{-1}$  with a weak shoulder at  $3400\text{ cm}^{-1}$ , whereas the signal intensity obtained with the presence of PEG-300 is much lower with a slightly stronger band at  $3400\text{ cm}^{-1}$ . The water signal decreases to almost zero when PEG-2000 is present. Different from free PEGs, for PEG-2000-AuNP, the observed SFG signal at  $3200\text{ cm}^{-1}$  is much stronger, indicating a majority of strongly hydrogen-bonded water at the interface. Therefore, the results obtained from the  $\text{CaF}_2$  surface without the proteins are consistent with those obtained from the protein surfaces.

Because PEG is a hydrogen-bond acceptor, it is plausible to envision that upon adding the PEG chains into water, the hydrogen bonding of water molecules will be broken to liberate free water molecules, which resembles hydrogen-bond disruption of chaotropic ions. On one hand, it weakens the hydration of proteins and thus facilitates the hydrophobic interaction between the proteins and PEG chains, when free PEG chains are present in water. In the case of PEG chains tethered on solid surfaces, on the other hand, the hydrophobic interaction between the PEG chains and the proteins is inhibited, and, at the same time, the liberated water molecules may interact with the proteins via hydrogen bonding, which may offset the hydrogen-bond disruption impact of the PEG chains on the hydration of the proteins. Overall, one can conclude that the impact of PEG chains on the hydration of proteins is strongly dependent on their forms present in water (Figure 4). This dependence can well account for the difference between free PEG chains, pOEGMA brushes grafted on solid surfaces, and PEG-2000-AuNPs when they interact with the proteins. It also accounts for the nonfouling effect of pOEGMA brush surfaces and for the enhancement of protein hydration by

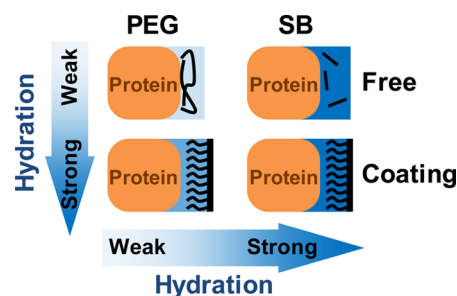


**Figure 4.** Schematic depiction of different hydration behaviors of PEG and SB (free or surface-bound) in contact with proteins.

PEG-2000-AuNPs (e.g., lysozyme in this work). In contrast to PEG, the interaction of SB with water and proteins is determined by its zwitterionic nature; it is always strongly hydrogen-bonded with water no matter whether it is present in water as free molecules or as surface-bound pSBMA coatings. The hydration of SB coatings (e.g., pSBMA) should be stronger than that of PEG (e.g., pOEGMA), because the latter can be disturbed by proteins.

## CONCLUSION

In this work, the surface hydration behaviors of pSBMA and pOEGMA were in situ probed in contact with protein solutions using SFG spectroscopy. The polymer surfaces were well ordered in air and water, and most of the water molecules at the polymer/water interface were strongly hydrogen-bonded. The hydration layer at the pSBMA surface was not affected by proteins, whereas that at the pOEGMA surface was considerably disturbed. The effects of free SB and PEG on the surface hydration of proteins were also investigated. Whereas water was strongly bonded at the protein surfaces with the presence of free SB molecules in solution, a significant amount of weakly hydrogen-bonded water molecules was observed at the interface between proteins and free PEG solutions. Different from free PEG, when the proteins were in contact with PEG-coated gold nanoparticles, a majority of strongly hydrogen-bonded water was observed, which is similar to the pOEGMA surface. In summary, the study on the surface hydration of both polymers and proteins suggests that for PEG-coated surfaces and nanoparticles, although surface hydration is disrupted by proteins to a certain degree, it is still relatively strong and resists protein adsorption. However, free PEG binds to proteins, reducing their hydration significantly. For SB-coated surfaces or free SB, surface hydration remains strong in contact with proteins.

## ASSOCIATED CONTENT

### Supporting Information

Static water contact angles for pSBMA and pOEGMA prepared in this work; adsorption of FITC-BSA on pSBMA and pOEGMA surfaces detected by fluorescence spectroscopy with a silica surface as a control; water contact angles on the surfaces of  $\text{CaF}_2$ , d8PS- $\text{CaF}_2$ , and proteins-d8PS- $\text{CaF}_2$ ; molecular weight and isoelectric point of the proteins; SFG spectra of pSBMA and pOEGMA in contact with water, an aqueous solution of NaCl and  $\text{NaH}_2\text{C}_6\text{H}_5\text{O}_7$  (monosodium citrate), and PBS; SFG spectra of pSBMA and pOEGMA in contact with water before and after contacting lysozyme and fibrinogen solutions and rinsing with water; SFG spectra of a silica surface in air and water before, during, and after contacting the protein solutions; SFG spectra of BSA, lysozyme, and fibrinogen adsorbed on d8-PS coatings in contact with water and aqueous solutions of SB and  $(\text{NH}_4)_2\text{SO}_4$ ; and SFG spectra collected at a  $\text{CaF}_2$  prism surface in contact with water and aqueous solutions of SB, PEG-300, PEG-2000, and PEG-2000-AuNPs. The Supporting Information is available free of charge on the ACS Publications website at DOI: 10.1021/acsami.5b05627.

## AUTHOR INFORMATION

### Corresponding Authors

\*Fax: (734) 647-4865. E-mail: zhanc@umich.edu.

\*Fax: (206) 685-3451. E-mail: sjiang@u.washington.edu.

\*Fax: 61-8-8302-3683. E-mail: dayang.wang@unisa.edu.au.

## Notes

The authors declare no competing financial interest.

## ACKNOWLEDGMENTS

This research is supported by the Office of Naval Research (N00014-12-1-0452, N00014-14-1-0090, N00014-15-1-2277, and N00014-15-1-2113).

## REFERENCES

- (1) Rosenhahn, A.; Schilp, S.; Kreuzer, H. J.; Grunze, M. The Role of "Inert" Surface Chemistry in Marine Biofouling Prevention. *Phys. Chem. Chem. Phys.* **2010**, *12*, 4275–4286.
- (2) Grozea, C. M.; Walker, G. C. Approaches in Designing Non-toxic Polymer Surfaces to Deter Marine Biofouling. *Soft Matter* **2009**, *5*, 4088–4100.
- (3) Welch, M.; Rastogi, A.; Ober, C. Polymer Brushes for Electrochemical Biosensors. *Soft Matter* **2011**, *7*, 297–302.
- (4) Callow, J. A.; Callow, M. E. Trends in the Development of Environmentally Friendly Fouling-resistant Marine Coatings. *Nat. Commun.* **2011**, *2*, 244.
- (5) Wei, Q.; Becherer, T.; Angioletti-Uberti, S.; Dzubiella, J.; Wischke, C.; Neffe, A. T.; Lendlein, A.; Ballauff, M.; Haag, R. Protein Interactions with Polymer Coatings and Biomaterials. *Angew. Chem., Int. Ed.* **2014**, *53*, 8004–8031.
- (6) Schlenoff, J. B. Zwitterion: Coating Surfaces with Zwitterionic Functionality to Reduce Nonspecific Adsorption. *Langmuir* **2014**, *30*, 9625–9636.
- (7) Jiang, S. Y.; Cao, Z. Q. Ultralow-Fouling, Functionalizable, and Hydrolyzable Zwitterionic Materials and Their Derivatives for Biological Applications. *Adv. Mater.* **2010**, *22*, 920–932.
- (8) Ma, H. W.; Hyun, J.; Stiller, P.; Chilkoti, A. Non-Fouling" Oligo(ethylene glycol)- Functionalized Polymer Brushes Synthesized by Surface-Initiated Atom Transfer Radical Polymerization. *Adv. Mater.* **2004**, *16*, 338–341.
- (9) Chen, S. F.; Li, L. Y.; Zhao, C.; Zheng, J. Surface Hydration: Principles and Applications toward Low-fouling/nonfouling Biomaterials. *Polymer* **2010**, *51*, 5283–5293.
- (10) Leung, B. O.; Yang, Z.; Wu, S. S. H.; Chou, K. C. Role of Interfacial Water on Protein Adsorption at Cross-Linked Polyethylene Oxide Interfaces. *Langmuir* **2012**, *28*, 5724–5728.
- (11) Galvin, C. J.; Dimitriou, M. D.; Satija, S. K.; Genzer, J. Swelling of Polyelectrolyte and Polyzwitterion Brushes by Humid Vapors. *J. Am. Chem. Soc.* **2014**, *136*, 12737–12745.
- (12) Gunkel, G.; Huck, W. T. S. Cooperative Adsorption of Lipoprotein Phospholipids, Triglycerides, and Cholesteryl Esters Are a Key Factor in Nonspecific Adsorption from Blood Plasma to Antifouling Polymer Surfaces. *J. Am. Chem. Soc.* **2013**, *135*, 7047–7052.
- (13) Shao, Q.; He, Y.; White, A. D.; Jiang, S. Y. Different Effects of Zwitterion and Ethylene Glycol on Proteins. *J. Chem. Phys.* **2012**, *136*, 225101–6.
- (14) Keefe, A. J.; Jiang, S. Y. Poly(zwitterionic)protein Conjugates Offer Increased Stability without Sacrificing Binding Affinity or Bioactivity. *Nat. Chem.* **2011**, *4*, 59–63.
- (15) Welscher, K.; McManus, S. A.; Hsia, C.-H.; Yin, S.; Yang, H. Discovery of Protein- and DNA-Imperceptible Nanoparticle Hard Coating Using Gel-Based Reaction Tuning. *J. Am. Chem. Soc.* **2015**, *137*, 580–583.
- (16) Zhang, L.; Cao, Z. Q.; Bai, T.; Carr, L.; Ella-Menye, J. R.; Irvin, C.; Ratner, B. D.; Jiang, S. Y. Zwitterionic Hydrogels Implanted in Mice Resist the Foreign-body Reaction. *Nat. Biotechnol.* **2013**, *31*, 553–556.
- (17) Yang, W.; Liu, S. J.; Bai, T.; Keefe, A. J.; Zhang, L.; Ella-Menye, J. R.; Li, Y. T.; Jiang, S. Y. Poly(carboxybetaine) Nanomaterials Enable Long Circulation and Prevent Polymer-Specific Antibody Production. *Nano Today* **2014**, *9*, 10–16.
- (18) Lambert, A. G.; Davies, P. B.; Neivandt, D. J. Implementing the Theory of Sum Frequency Generation Vibrational Spectroscopy: A Tutorial Review. *Appl. Spectrosc. Rev.* **2005**, *40*, 103–145.
- (19) Shen, Y. R. Basic Theory of Surface Sum-Frequency Generation. *J. Phys. Chem. C* **2012**, *116*, 15505–15509.
- (20) Perry, A.; Neipert, C.; Space, B.; Moore, P. B. Theoretical Modeling of Interface Specific Vibrational Spectroscopy: Methods and Applications to Aqueous Interfaces. *Chem. Rev.* **2006**, *106*, 1234–1258.
- (21) Chen, Z. Investigating Buried Polymer Interfaces Using Sum Frequency Generation Vibrational Spectroscopy. *Prog. Polym. Sci.* **2010**, *35*, 1376–1402.
- (22) Roy, S.; Covert, P. A.; FitzGerald, W. R.; Hore, D. K. Biomolecular Structure at Solid–Liquid Interfaces As Revealed by Nonlinear Optical Spectroscopy. *Chem. Rev.* **2014**, *114*, 8388–8415.
- (23) Yan, E. C. Y.; Fu, L.; Wang, Z. G.; Liu, W. Biological Macromolecules at Interfaces Probed by Chiral Vibrational Sum Frequency Generation Spectroscopy. *Chem. Rev.* **2014**, *114*, 8471–8498.
- (24) Hankett, J. M.; Liu, Y. W.; Zhang, X. X.; Zhang, C.; Chen, Z. Molecular Level Studies of Polymer Behaviors at the Water Interface Using Sum Frequency Generation Vibrational Spectroscopy. *J. Polym. Sci., Part B: Polym. Phys.* **2013**, *51*, 311–328.
- (25) Ye, S. J.; Liu, G. M.; Li, H. C.; Chen, F. G.; Wang, X. W. Effect of Dehydration on the Interfacial Water Structure at a Charged Polymer Surface: Negligible  $\chi^{(3)}$  Contribution to Sum Frequency Generation Signal. *Langmuir* **2012**, *28*, 1374–1380.
- (26) Gopalakrishnan, S.; Liu, D. F.; Allen, H. C.; Kuo, M.; Shultz, M. J. Vibrational Spectroscopic Studies of Aqueous Interfaces: Salts, Acids, Bases, and Nanodrops. *Chem. Rev.* **2006**, *106*, 1155–1175.
- (27) Nihonyanagi, S.; Ishiyama, T.; Lee, T.; Yamaguchi, S.; Bonn, M.; Morita, A.; Tahara, T. Unified Molecular View of the Air/Water Interface Based on Experimental and Theoretical  $\chi^{(2)}$  Spectra of an Isotopically Diluted Water Surface. *J. Am. Chem. Soc.* **2011**, *133*, 16875–16880.
- (28) Stiofkin, I. V.; Weeraman, C.; Pieniazek, P. A.; Shalhout, F. Y.; Skinner, J. L.; Benderskii, A. V. Hydrogen Bonding at the Water Surface Revealed by Isotopic Dilution Spectroscopy. *Nature* **2011**, *474*, 192–195.
- (29) Scatena, L. F.; Brown, M. G.; Richmond, G. L. Water at Hydrophobic Surfaces: Weak Hydrogen Bonding and Strong Orientation Effects. *Science* **2001**, *292*, 908–912.
- (30) Ji, N.; Ostroverkhov, V.; Tian, C. S.; Shen, Y. R. Characterization of Vibrational Resonances of Water-Vapor Interfaces by Phase-Sensitive Sum-Frequency Spectroscopy. *Phys. Rev. Lett.* **2008**, *100*, 096102.
- (31) Ma, H. W.; Li, D. J.; Sheng, X.; Zhao, B.; Chilkoti, A. Protein-resistant Polymer Coatings on Silicon Oxide by Surface-initiated Atom Transfer Radical Polymerization. *Langmuir* **2006**, *22*, 3751–3756.
- (32) Yang, W.; Chen, S. F.; Cheng, G.; Vaisocherova, H.; Xue, H.; Li, W.; Zhang, J. L.; Jiang, S. Y. Film Thickness Dependence of Protein Adsorption from Blood Serum and Plasma onto Poly(sulfobetaine)-grafted Surfaces. *Langmuir* **2008**, *24*, 9211–9214.
- (33) Leng, C.; Han, X. F.; Shao, Q.; Zhu, Y. H.; Li, Y. T.; Jiang, S. Y.; Chen, Z. In Situ Probing of the Surface Hydration of Zwitterionic Polymer Brushes: Structural and Environmental Effects. *J. Phys. Chem. C* **2014**, *118*, 15840–15845.
- (34) Wang, J.; Chen, C. Y.; Buck, S. M.; Chen, Z. Molecular Chemical Structure on Poly(methyl methacrylate) (PMMA) Surface Studied by Sum Frequency Generation (SFG) Vibrational Spectroscopy. *J. Phys. Chem. B* **2001**, *105*, 12118–12125.
- (35) Holmlin, R. E.; Chen, X.; Chapman, R. G.; Takayama, S.; Whitesides, G. M. Zwitterionic SAMs that Resist Nonspecific Adsorption of Protein from Aqueous Buffer. *Langmuir* **2001**, *17*, 2841–2850.
- (36) Sundaram, H. S.; Ella-Menye, J.-R.; Brault, N. D.; Shao, Q.; Jiang, S. Y. Reversibly Switchable Polymer with Cationic/Zwitterionic/Anionic Behavior Through Synergistic Protonation and Deprotonation. *Chem. Sci.* **2014**, *5*, 200–205.

- (37) Bernards, M. T.; Cheng, G.; Zhang, Z.; Chen, S. F.; Jiang, S. Y. Nonfouling Polymer Brushes via Surface-Initiated, Two-Component Atom Transfer Radical Polymerization. *Macromolecules* **2008**, *41*, 4216–4219.
- (38) Chen, S. F.; Jiang, S. Y. A New Avenue to Nonfouling Materials. *Adv. Mater.* **2008**, *20*, 335–338.
- (39) Mi, L.; Bernards, M. T.; Cheng, G.; Yu, Q. M.; Jiang, S. Y. pH Responsive Properties of Non-fouling Mixed-charge Polymer Brushes based on Quaternary Amine and Carboxylic Acid Monomers. *Biomaterials* **2010**, *31*, 2919–2925.
- (40) Azzaroni, O.; Brown, A. A.; Huck, W. T. S. UCST Wetting Transitions of Polyzwitterionic Brushes Driven by Self-association. *Angew. Chem., Int. Ed.* **2006**, *45*, 1770–1774.
- (41) Huang, C.-J.; Li, Y. T.; Krause, J. B.; Brault, N. D.; Jiang, S. Y. Internal Architecture of Zwitterionic Polymer Brushes Regulates Nonfouling Properties. *Macromol. Rapid Commun.* **2012**, *33*, 1003–1007.
- (42) Li, L. Y.; Chen, S. F.; Zheng, J.; Ratner, B. D.; Jiang, S. Y. Protein Adsorption on Oligo(ethylene glycol)-Terminated Alkanethiolate Self-Assembled Monolayers: The Molecular Basis for Nonfouling Behavior. *J. Phys. Chem. B* **2005**, *109*, 2934–2941.
- (43) Yuan, J.; Huang, X.; Li, P.; Li, L.; Shen, J. Surface-initiated RAFT Polymerization of Sulfobetaine from Cellulose Membranes to Improve Hemocompatibility and Antibiofouling Property. *Polym. Chem.* **2013**, *4*, 5074–5085.
- (44) Nguyen, A. T.; Baggerman, J.; Paulusse, J. M. J.; van Rijn, C. J. M.; Zuilhof, H. Stable Protein-Repellent Zwitterionic Polymer Brushes Grafted from Silicon Nitride. *Langmuir* **2011**, *27*, 2587–2594.
- (45) Kobayashi, M.; Terayama, Y.; Yamaguchi, H.; Terada, M.; Murakami, D.; Ishihara, K.; Takahara, A. Wettability and Antifouling Behavior on the Surfaces of Superhydrophilic Polymer Brushes. *Langmuir* **2012**, *28*, 7212–7222.
- (46) Tang, L.; Lee, N. Y. A Facile Route for Irreversible Bonding of Plastic-PDMS Hybrid Microdevices at Room Temperature. *Lab Chip* **2010**, *10*, 1274–1280.
- (47) Wu, J.; Lee, N. Y. One-step Surface Modification for Irreversible Bonding of Various Plastics with a Poly(dimethylsiloxane) Elastomer at Room Temperature. *Lab Chip* **2014**, *14*, 1564–1571.
- (48) Cantini, M.; Sousa, M.; Moratal, D.; Mano, J. F.; Salmeron-Sanchez, M. Non-monotonic Cell Differentiation Pattern on Extreme Wettability Gradients. *Biomater. Sci.* **2013**, *1*, 202–212.
- (49) Zhang, Z.; Chen, S. F.; Chang, Y.; Jiang, S. Y. Surface Grafted Sulfobetaine Polymers via Atom Transfer Radical Polymerization as Superlow Fouling Coatings. *J. Phys. Chem. B* **2006**, *110*, 10799–10804.
- (50) Ladd, J.; Zhang, Z.; Chen, S. F.; Hower, J. C.; Jiang, S. Y. Zwitterionic Polymers Exhibiting High Resistance to Nonspecific Protein Adsorption from Human Serum and Plasma. *Biomacromolecules* **2008**, *9*, 1357–1361.
- (51) Kim, J.; Somorjai, G. A. Molecular Packing of Lysozyme, Fibrinogen, and Bovine Serum Albumin on Hydrophilic and Hydrophobic Surfaces Studied by Infrared-Visible Sum Frequency Generation and Fluorescence Microscopy. *J. Am. Chem. Soc.* **2003**, *125*, 3150–3158.
- (52) Wang, J.; Buck, S. M.; Even, M. A.; Chen, Z. Molecular Responses of Proteins at Different Interfacial Environments Detected by Sum Frequency Generation Vibrational Spectroscopy. *J. Am. Chem. Soc.* **2002**, *124*, 13302–13305.
- (53) Wu, J.; Wang, Z.; Lin, W. F.; Chen, S. F. Investigation of the Interaction Between Poly(ethylene glycol) and Protein Molecules Using Low Field Nuclear Magnetic Resonance. *Acta Biomater.* **2013**, *9*, 6414–6420.